Carbazole-Embedded *p*-Benziporphyrinoid: Synthesis, Structure and Reversible Chemodosimeter for Mercury(II) Ion

Athira Naniyil, Naveen Koroth Valappil, Alex P. Andrews and Sabapathi Gokulnath*

Indian Institute of Science Education and Research Thiruvananthapuram, Kerala-695551, India.

SI. No.	**Contents**	**Page No.**
1.	General Information	2
2.	Synthetic Procedures and Compound Data	3-4
3.	High-Resolution APCI-TOF Mass Spectra	5-6
4.	NMR Spectra	7-11
5.	UV/Vis Absorption Spectra	12-16
6.	X-ray Crystallographic Data	17-19
7.	DFT Calculations	19-34
8.	Supporting References	34-35

1. General Information

The reagents and materials for the synthesis were used as obtained from Sigma -Aldrich chemical suppliers. All solvents were purified and dried by standard methods prior to use. Thin-layer chromatography (TLC) was carried out on aluminum sheets coated with silica gel 60 F254 (Merck 5554). Silica gel column chromatography was performed on Wakogel C-230 - 400 mesh. Alumina column chromatography was performed on Active alumina (basic). Recrystallized samples of porphyrinoids were utilized for all the spectroscopic measurements. The mass spectra were recorded with Bruker UltrafleXtreme MALDI-TOF mass spectrometer and the High-resolution mass spectra (HRMS) were recorded on Q Exactive TM-Bench top-LC-HRMS mass spectrometer. ^{1}H NMR (500) and ^{13}C NMR (126 MHz) spectra were recorded on BRUKER Avance 500 MHz spectrometer, and chemical shifts were reported as the delta scale in ppm relative to $CHCl_3$ as an internal reference for ^{1}H (7.26 ppm) and for ^{13}C (77.20 ppm). The optical absorption spectra were recorded on a Shimadzu (Model UV-3600) spectrophotometer. Concentrations of the solutions are *ca*. to be 1×10^{-6} M.

Theoretical Calculations: All calculations were carried out using the Gaussian 16 program package.[S1] Calculations were performed by the density functional theory (DFT) method with restricted B3LYP (Becke's three-parameter hybrid exchange functional and the Lee-Yang-Parr correlation functional)[S2] level, employing a basis sets 6-311G(d). Vertical electronic excitations were based on B3LYP-optimized geometries using the time-dependent density functional theory (TD-DFT) formalism.[S3] The nucleus-independent chemical shift (NICS (0)) values were determined at the mean position of the core atoms of the optimized structures by the B3LYP/6-311G(d) method. Anisotropy of the current-induced density (ACID) plots were obtained by employing the continuous set of gauge transformations method to calculate the current densities, and the results were plotted by using POVRAY.

X-ray Crystal Structure Analysis: Single crystals were grown by slow vapour diffusion of hexane into a $CHCl_3$ solution of **1**; and methanol into a $CHCl_3$ solution of **1-Hg**. Single crystals were mounted at 140 K on a three-circle Bruker SMART APEX CCD area detector system under a Mo-Kα (λ = 0.71073 Å) graphite monochromatic X-ray beam. The structures were solved by direct methods and least-square refinement on F2 for **1** by using SHELXS-97.[S4] All non-hydrogen atoms were refined anisotropically. The hydrogen atoms were included in the structure factor calculation by using a riding model. The solvent molecule that could not be identified or modified in **1** was fixed and eventually squeezed using PLATON. [S5] The crystallographic parameters, data collection, and structure refinement of **1** and **1-Hg** are summarized in Table S6-1.

2. Synthetic Procedures and Compound Data

Synthesis of 1,8-dibromo-3,6-di-*tert*-butyl-9*H*-carbazole **2** was accomplished by slightly modifying the previously reported procedure.[S6]

Synthesis of the starting material 2: 3,6-di-*tert*-butyl-9*H*-carbazole (1.52 g, 5.4 mmol), and 150 ml glacial acetic acid were taken in an oven-dried two-neck round-bottom flask. To the above solution 0.62 mL of Br_2 (12 mmol) was added dropwise. The solution is allowed to stir for 1 h at room temperature. The reaction mixture was treated with cold water after the complete disappearance of the starting material. Then, the white precipitate formed was collected via vacuum filtration. The crude sample was subjected to column chromatography (silica gel, Pet Ether), and the product 1,8-dibromo-3,6-di-*tert*-butyl-9*H*-carbazole **2** was collected as a white solid in 80% (1.89 g) yield.

Synthesis of 3: Compound **2** (500 mg, 1.14 mmol), N-(*tert*-butoxycarbonyl)-pyrrole-2-boronic acid (975 mg, 4.57 mmol), and $PdCl_2(PPh_3)_2$ (161 mg, 0.229 mmol) were taken in a oven-dried two neck round-bottom flask fitted with a condenser. This was subjected to a vacuum for 15 min, following which 40 mL of DMF and 2 M aqueous K_2CO_3 (3.15 g, 22.79 mmol) were added. The solution is purged with argon for 10 min and then refluxed for 12 h at 145 °C using an oil bath. The reaction mixture was quenched with water after complete disappearance of starting material. Then, the organic layer was extracted with CH_2Cl_2 and solvent was removed on a rotary evaporator. The crude sample was subjected to column chromatography (silica gel, 50% CH_2Cl_2: Pet Ether), and the product 1,8-Di(-1*H*-pyrrole)-3,6-di-*tert*-butyl)-9*H*-carbazole **3** was collected as a pale-grey solid in 70% (328 mg) yield.

Synthesis of 4: To a 250 mL two-neck round bottom flask containing 1,4-Benzenedicarboxaldehyde (1.0 g, 6.09 mmol), 100 mL of THF was added followed by the dropwise addition of 12 mL of 2-Mesitylmagnesium bromide (54 mmol). The reaction mixture was stirred under Ar atmosphere for 16 h at room temperature. The reaction mixture was quenched with water after complete disappearance of starting material. Then, the organic layer was extracted with $CHCl_3$ and solvent was removed on a rotary evaporator to obtain **4** as a white solid in a quantitative yield.

Synthesis of 1: To a 250 mL two-neck round bottom flask containing compound **3** (100 mg, 0.244 mmol) and 1,4-phenylenebis(mesitylmethanol) **4** (92 mg, 0.244 mmol), 100 ml CH_2Cl_2

was added and stirred under Ar atmosphere under dark. *p*-toluenesulfonic acid (*p*-TsOH) (412 mg, 2.166 mmol) was added and the mixture was allowed to stir for 1 h. To the reaction mixture, 2,3-dichloro-5,6-dicyano-*p*-benzoquinone (DDQ) (100 mg, 0.44 mmol) was added and allowed to stir for further 10 min at room temperature. The entire reaction mixture was filtered through a pad of basic alumina and eluted with CH_2Cl_2 until the eluent was no longer dark. The resulting crude mixture was concentrated by rotary evaporator to give an orange solid. The crude solid was purified by silica column chromatography. The orange fraction eluted with 20% CH_2Cl_2/hexane provided **1** as an orange solid in 16.6% (30 mg) yield. ^{1}H NMR (500 MHz, $CDCl_3$) δ 10.06 (s, 1H), 8.41 (s, 2H), 8.24 (s, 2H), 7.64 (d, J = 4.9 Hz, 2H), 7.31 (s, 4H), 7.13 (d, J = 4.7 Hz, 2H), 7.03 (s, 4H), 2.40 (s, 6H), 2.25 (s, 12H), 1.57 (s, 18H). ^{13}C NMR (126 MHz, $CDCl_3$) δ 169.46, 156.54, 146.90, 140.69, 140.44, 136.96, 136.42, 135.11, 133.85, 133.28, 128.43, 127.39, 126.11, 124.62, 123.93, 117.73, 116.01, 33.69, 31.00, 20.18, 19.99. UV-Vis (CH_2Cl_2): λ_{max}/nm (ε [x 10^5 M^{-1} cm^{-1}]): 290 (28557), 375 (30918), 465 (8080). HRMS (APCI) *m/z*: $[M+H]^+$; calcd for: $C_{54}H_{53}N_3$: 744.4318; Found 744.4286, error = 4.29%

Synthesis of 1-Hg: To a 50 mL two-neck round bottom flask containing compound **1** (10 mg, 0.014 mmol) and mercury acetate (5.13 mg, 0.016 mmol), 16 mL of $CHCl_3$/CH_3OH (3:1) was added and stirred for 2 min at room temperature. The resulting crude mixture was concentrated by rotary evaporator to give a brown solid, which was purified by alumina column chromatography. The brown fraction eluted with 60% CH_2Cl_2/hexane provided **1-Hg** as a brown solid. ^{1}H NMR (500 MHz, $CDCl_3$) δ 8.58 (t, J = 3.3 Hz, 2H), 8.39 (t, J = 3.0 Hz, 2H), 7.89 (d, J = 4.9 Hz, 2H), 7.30 (s, 2H), 7.28 (s, 2H), 7.07 (s, 2H), 7.05 (s, 2H), 7.02 (s, 2H), 2.42 (s, 6H), 2.31 (s, 6H), 2.16 (s, 6H), 1.60 (s, 18H). UV-Vis (CH_2Cl_2): λ_{max}/nm (ε [x 10^5 M^{-1} cm^{-1}]): 302 (80373), 377 (75082), 548 (16912). HRMS (APCI) *m/z*: $[M+H]^+$; calcd for: $C_{54}H_{52}ClHgN_3$: 980.3634 ; Found 980.3634, error = 0.00%

1. High-Resolution APCI-TOF Mass Spectra

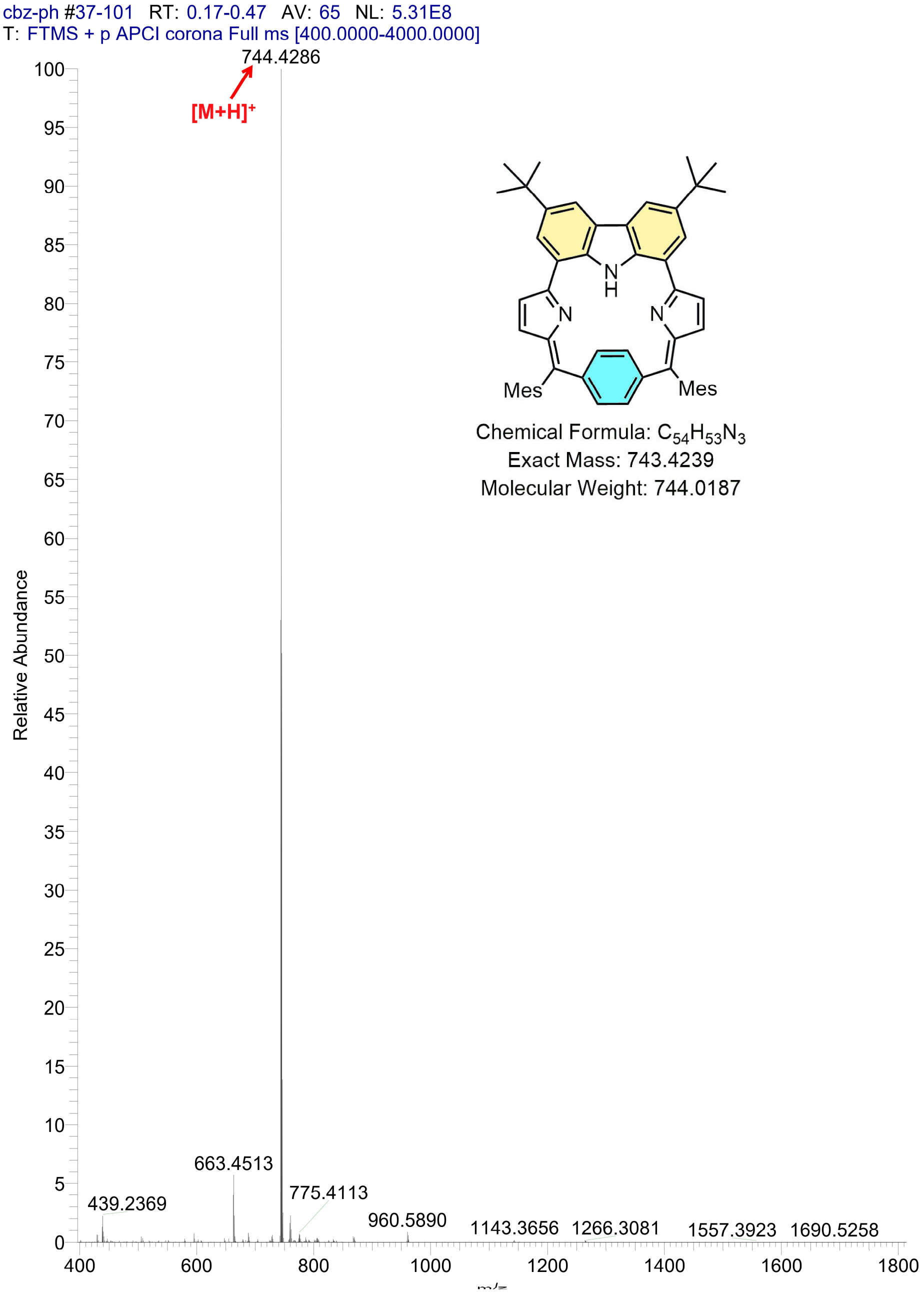

Figure S3-1. High-Resolution Mass Spectrum of **1**

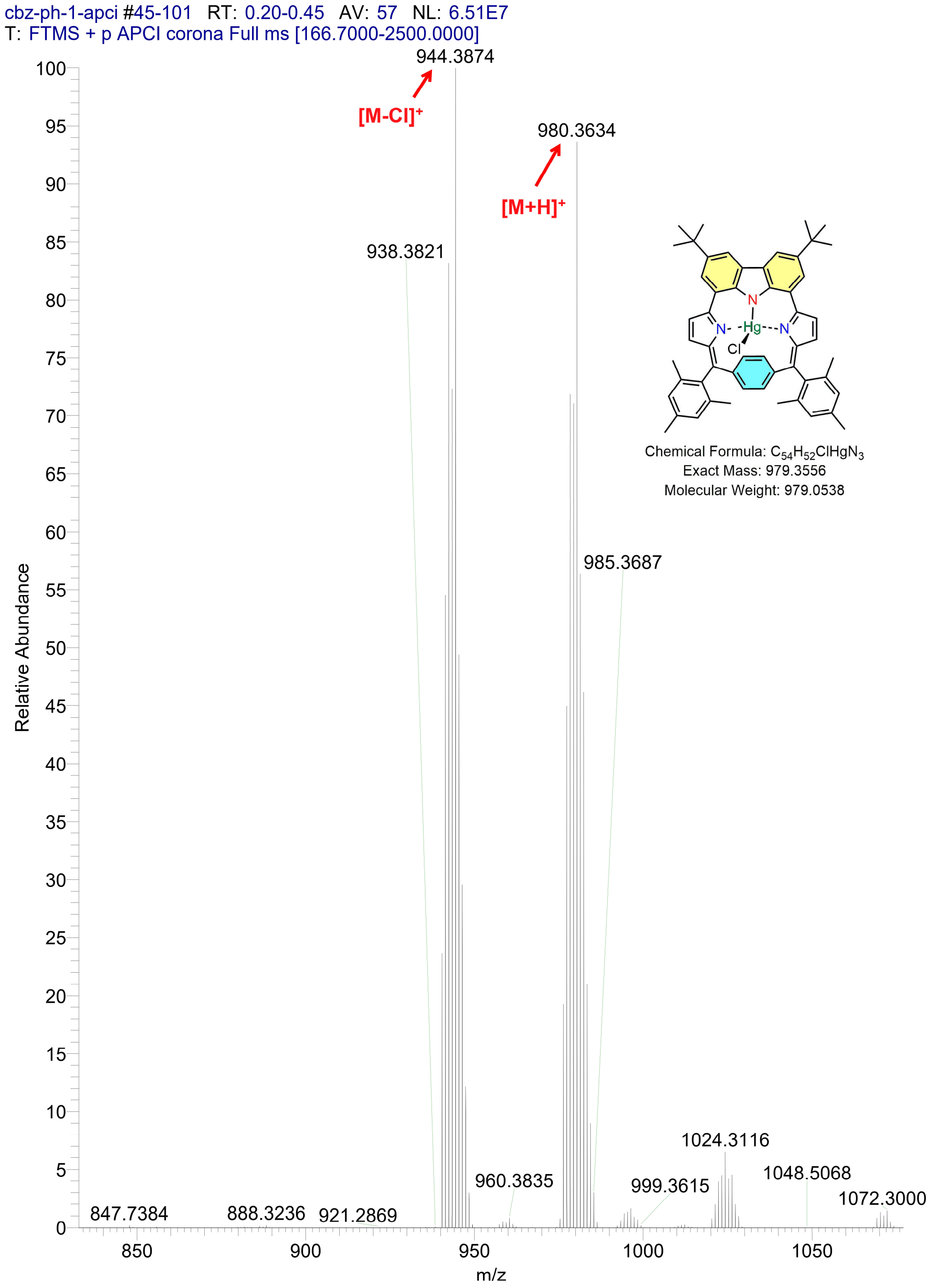

Figure S3-2. High Resolution Mass Spectrum of **1-Hg**

2. NMR Spectra

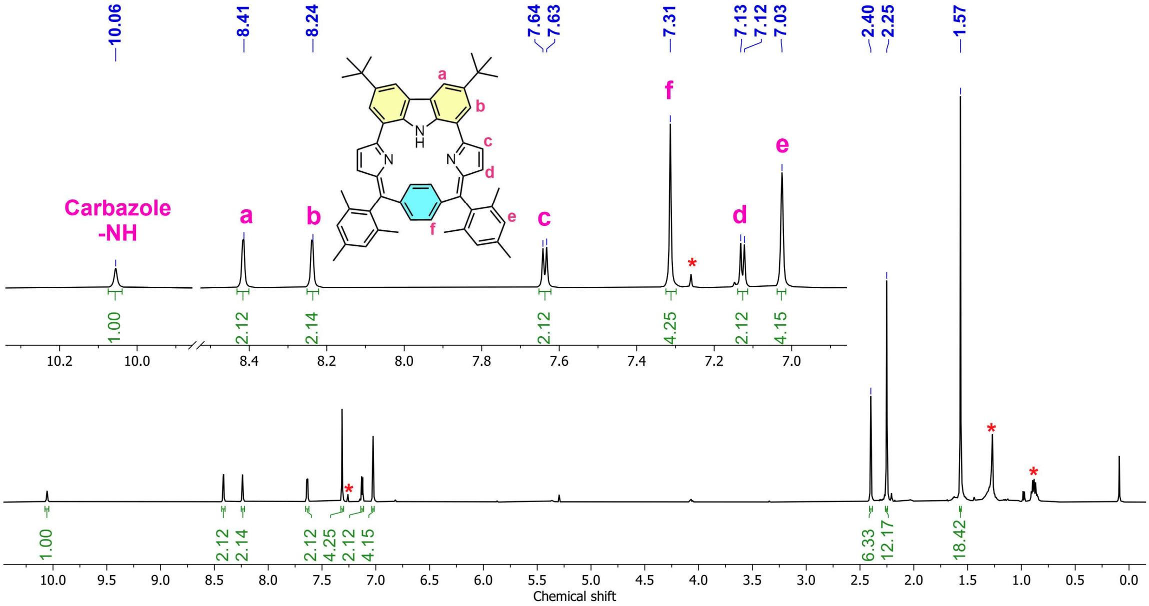

Figure S4-1. ^{1}H NMR of **1** recorded at 500 MHz in CDCl$_3$ at 298 K. Signals marked with (*) denotes residual solvents or impurities.

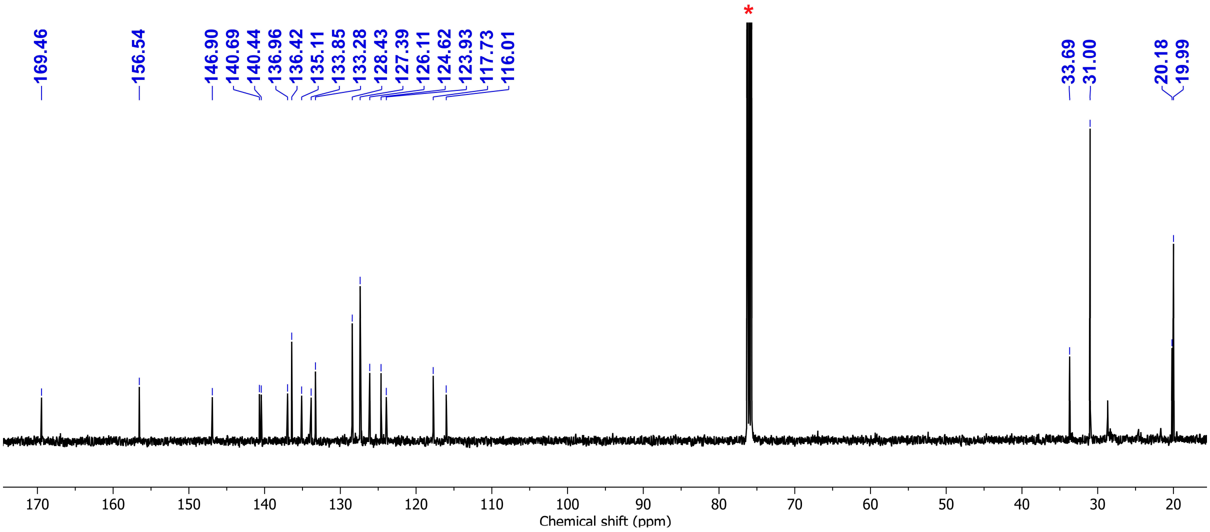

Figure S4-2. ^{13}C{1H} NMR spectrum of **1** recorded at 126 MHz in CDCl$_3$ at 298 K. Signals marked with (*) denotes residual solvents or impurities.

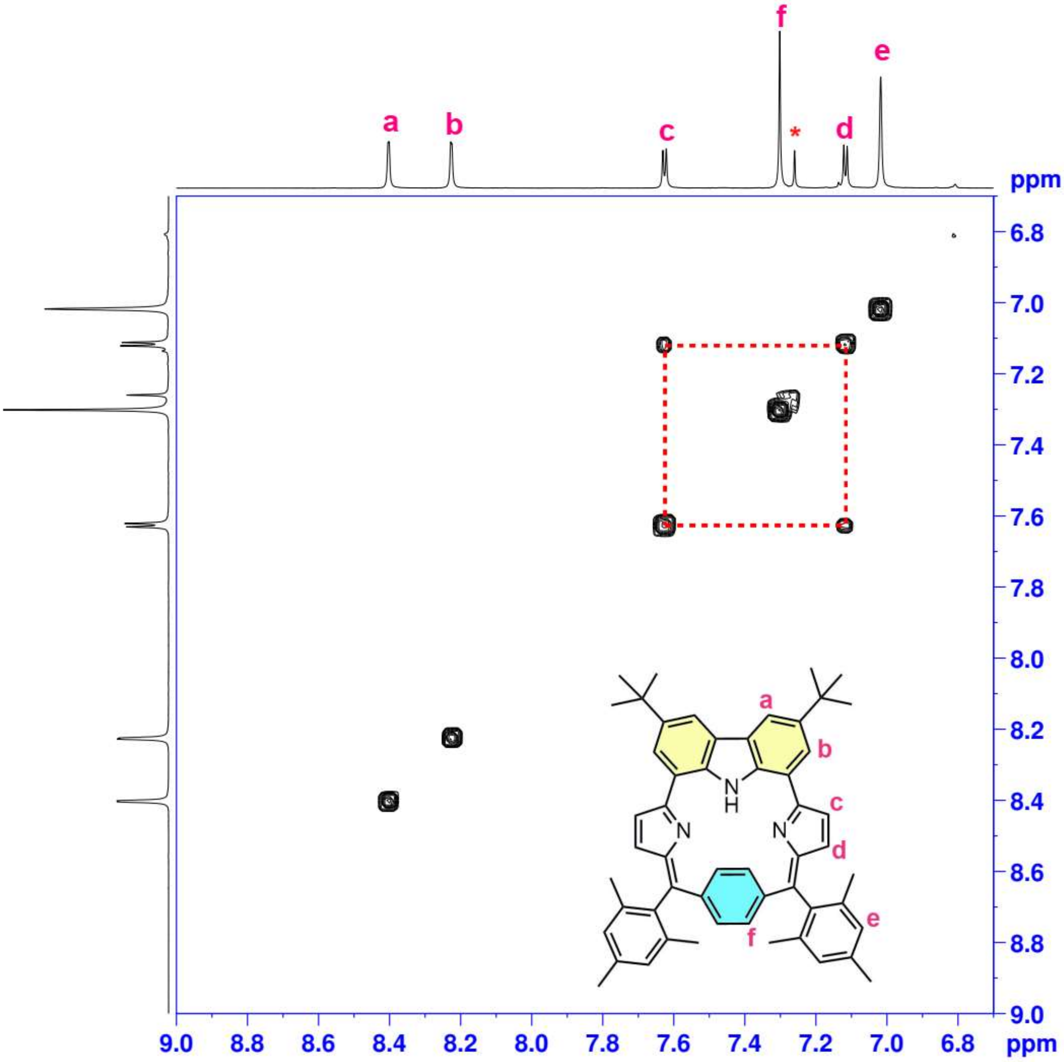

Figure S4-3. ^{1}H-^{1}H COSY spectrum of **1** recorded at 500 MHz in $CDCl_3$ at 298 K.

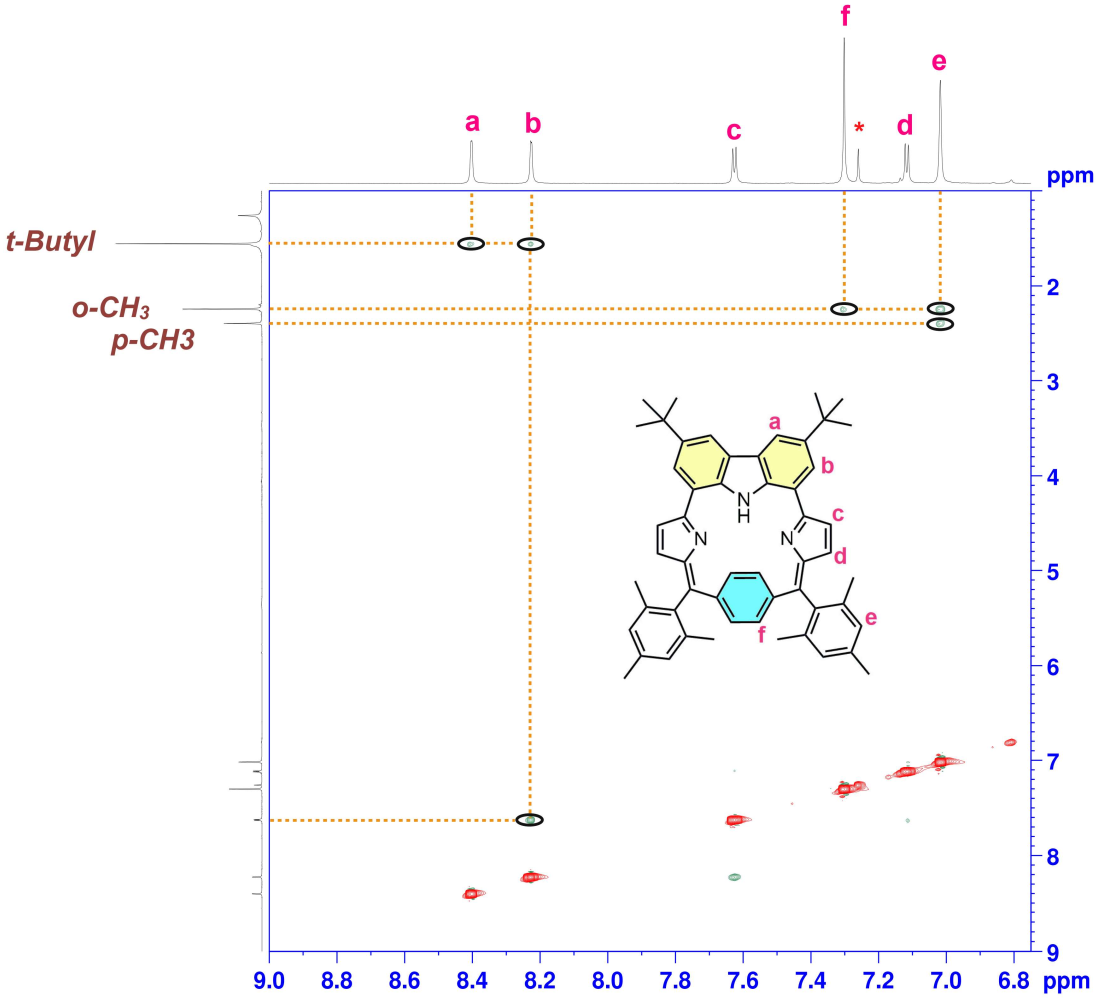

Figure S4-4. ^{1}H-^{1}H ROESY spectrum of **1** recorded at 500 MHz in $CDCl_3$ at 298 K.

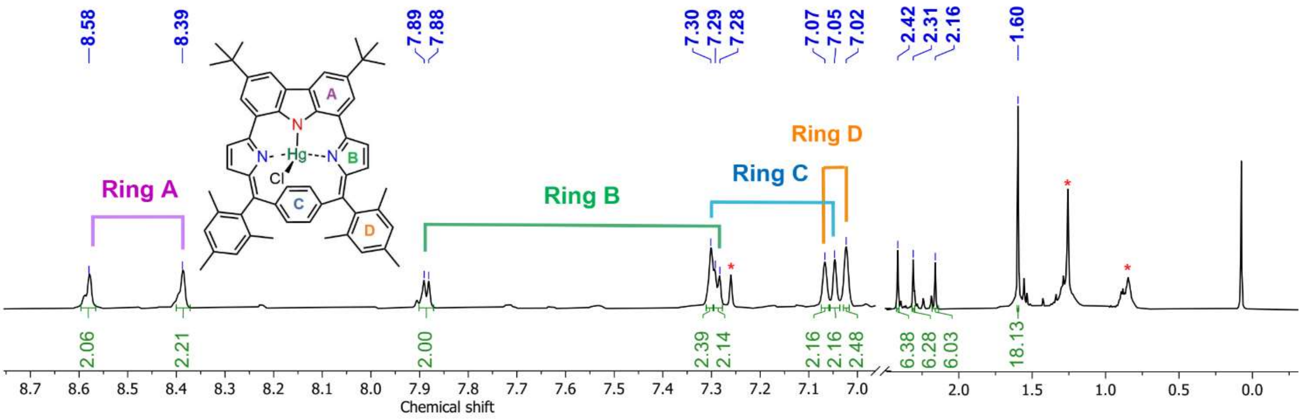

Figure S4-5. ^{1}H NMR of **1-Hg** recorded at 500 MHz in $CDCl_3$ at 298 K. Signals marked with (*) denotes residual solvents or impurities.

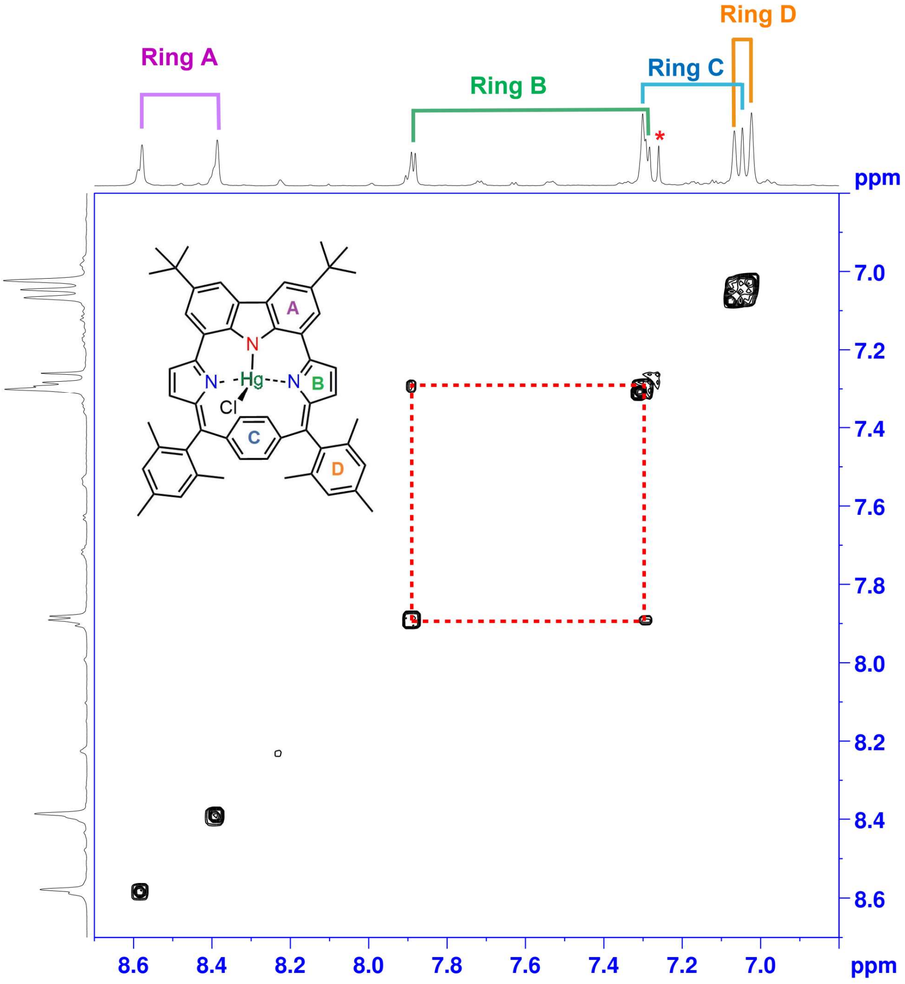

Figure S4-6. ^{1}H-^{1}H COSY spectrum of **1-Hg** recorded at 500 MHz in $CDCl_3$ at 298 K.

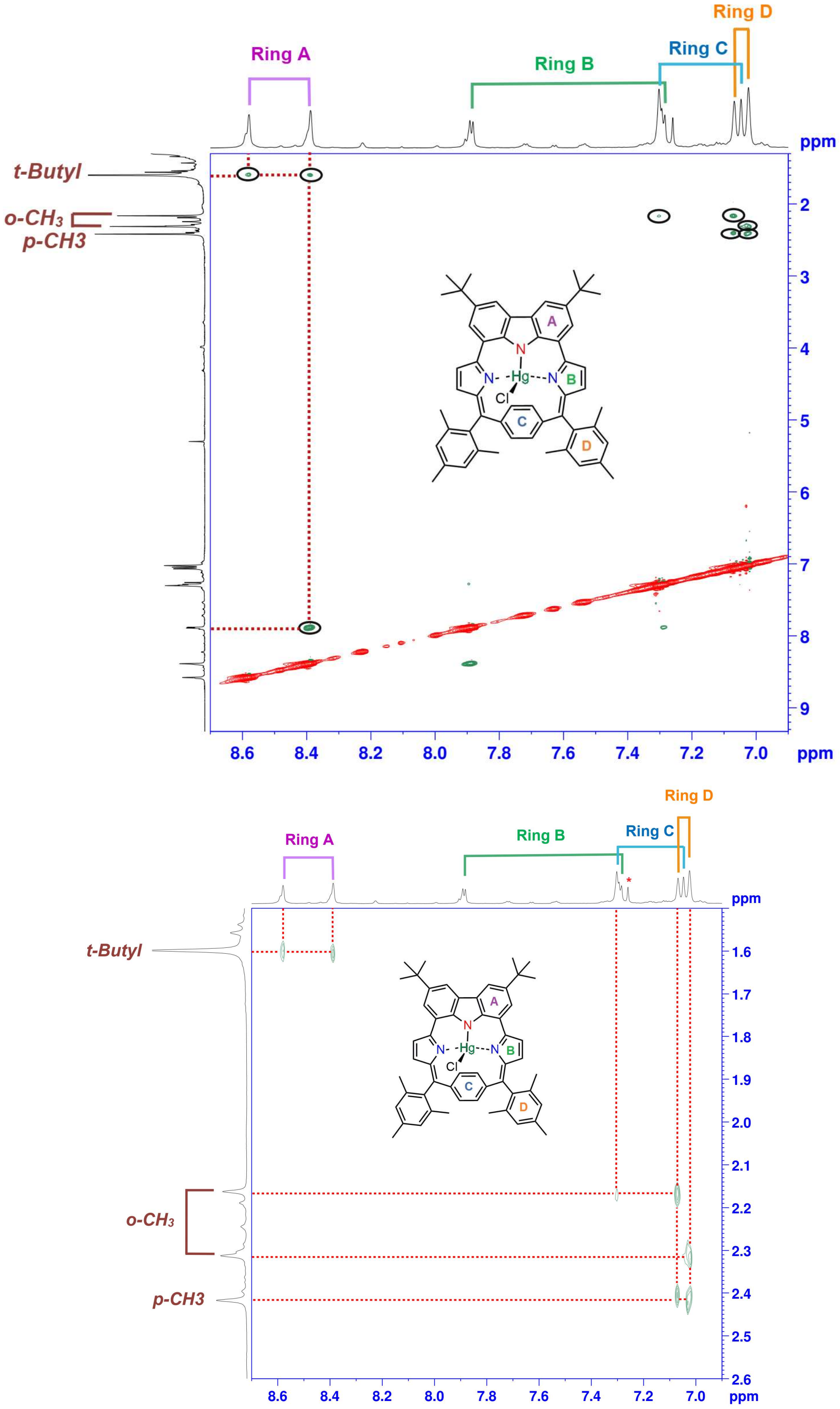

Figure S4-7. ^{1}H-^{1}H ROESY spectrum of **1-Hg** recorded at 500 MHz in CDCl$_3$ at 298 K

3. UV/Vis Absorption Spectra

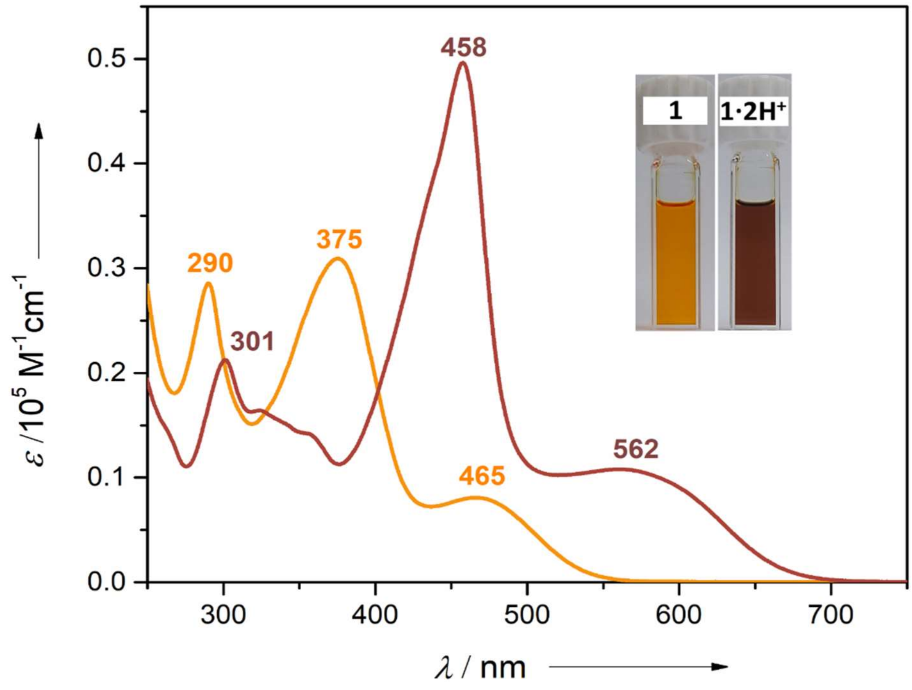

Figure S5-1. UV-Vis absorption spectra of **1** with its protonated form (diluted CF_3COOH used) recorded in CH_2Cl_2 at 298 K.

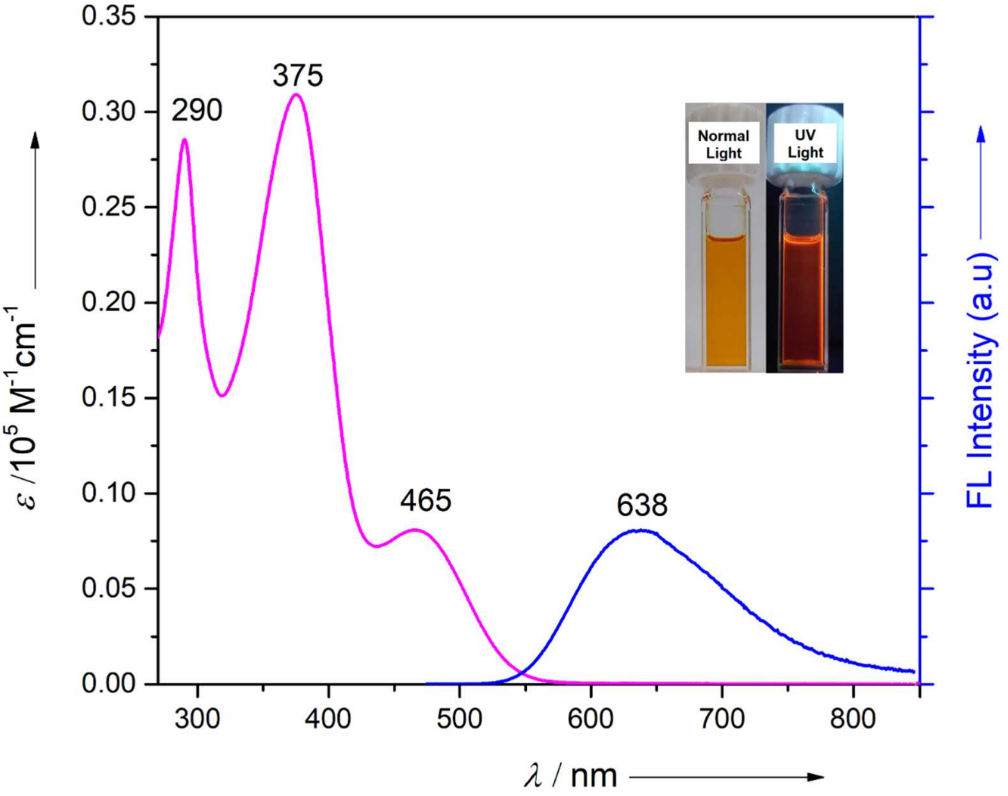

Figure S5-2. UV-Vis absorption and fluorescence spectrum of **1** recorded in CH_2Cl_2 at 298 K.

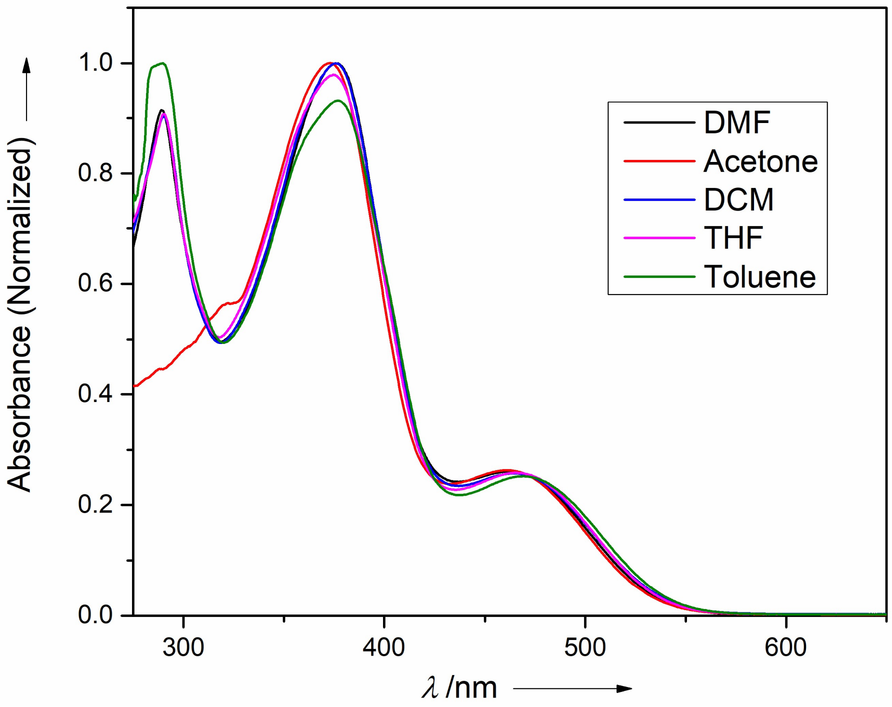

Figure S5-3. UV-Vis absorption spectra of **1** recorded in different solvents.

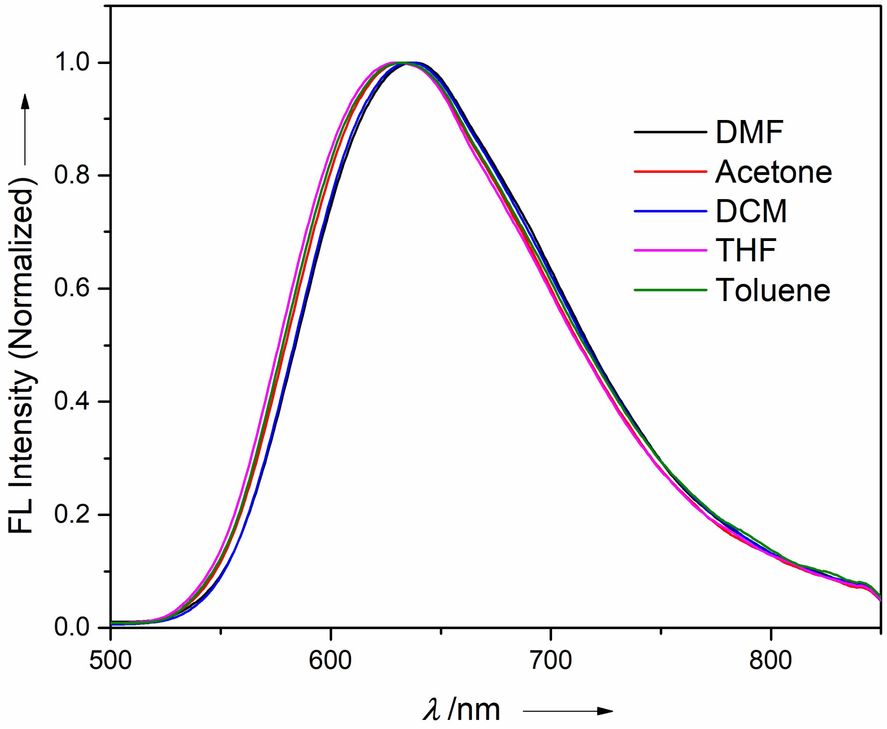

Figure S5-4. Emission spectra of **1** recorded in different solvents.

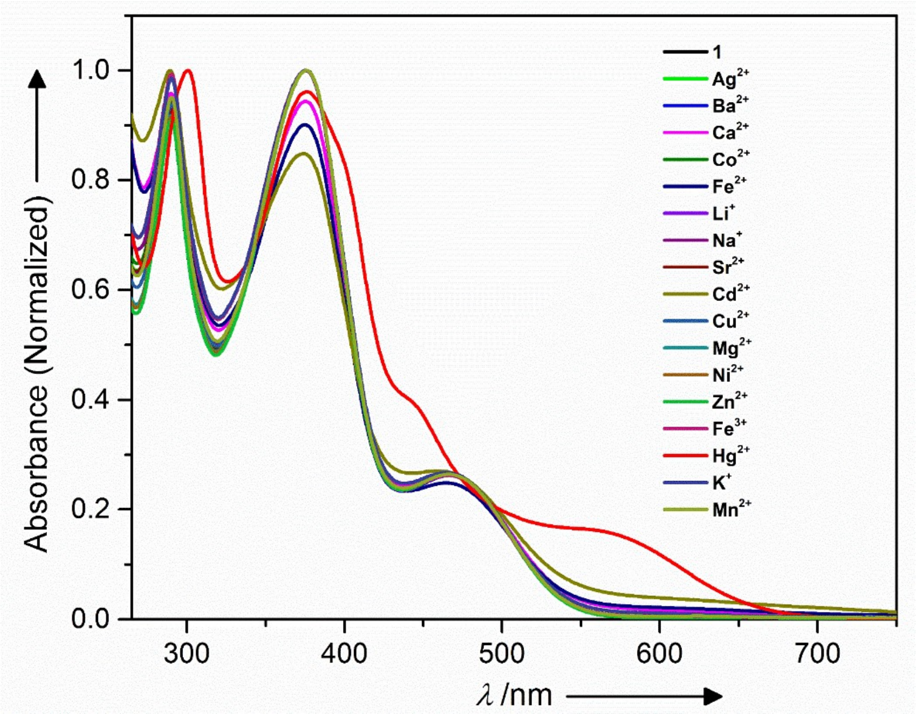

Figure S5-5. UV-Vis absorption changes of **1** (in CH_2Cl_2) upon addition of various metal ions.

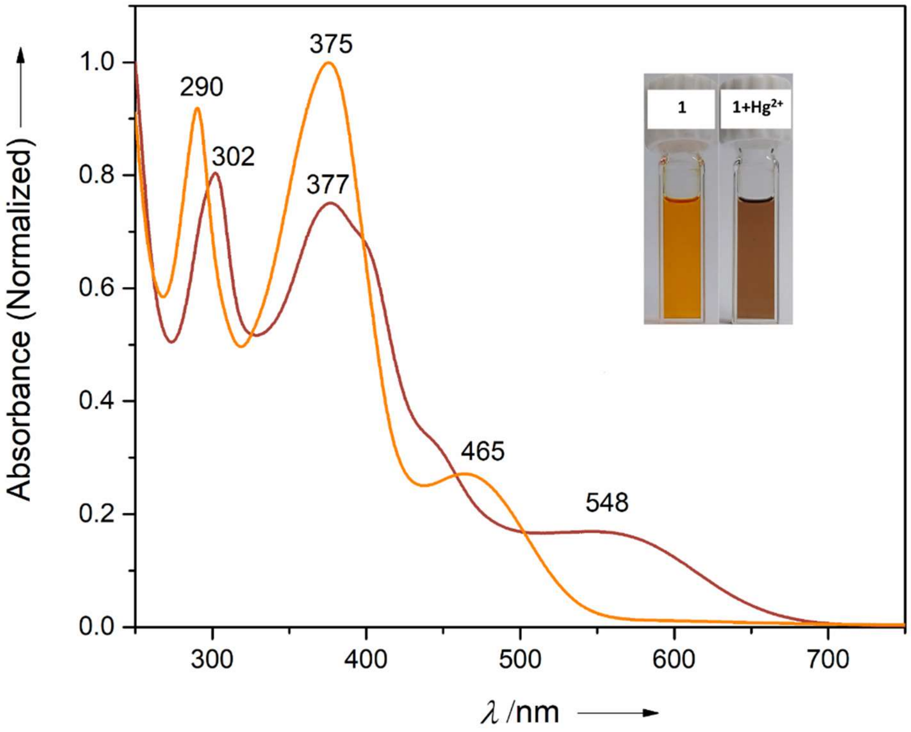

Figure S5-6. Comparative UV-Vis absorption spectra of **1** and **1-Hg** in CH_2Cl_2.

5.1. General procedure for obtaining Job's plot by fluorescence method:

Job's plot was used to identify the stoichiometry of the host-guest complex. Stock solutions of the sensor and Hg^{2+} were prepared in the order of 22 µM (in $CHCl_3$) and 1 mM (in CH_3OH), respectively. Using this, guest solutions with increasing amounts of Hg^{2+} were prepared as shown below (Column B).

Table S5-1: Concentrations and amount of sensor **1** and Hg^{2+} taken

Sl. No.	**A**	**B**	**C**
	Vol. of 1 mM Hg^{2+} taken (mL)	Conc. of Hg^{2+} (10^{-5} M) in 10 mL CH_3OH	Amount of Hg^{2+} present in 219 µL (nmol)
1.	No guest	No guest	No guest
2.	0.25	2.50	15.15
3.	0.50	5.00	30.30
4.	0.75	7.50	45.45
5.	1.00	10.00	60.60
6.	1.25	10.25	75.75
7.	1.50	10.50	90.90
8.	1.75	10.75	106.05
9.	2.00	20.00	121.20
10.	2.25	20.25	136.35
11.	2.50	20.50	151.50
12.	2.75	20.75	166.65
13.	3.00	30.00	181.80

The fluorescence in each case with a different host–guest ratio but equal volume was recorded. Every time 1 equivalent (60.60 nmol) of the sensor and increasing equivalents of Hg^{2+} (Table S5-1: column C) were added. Job's plots were drawn by plotting the intensity (I) *vs* X_{host} (I = emission intensity at 638 nm during titration and X_{host} is the mole fraction of the host in each case, respectively).

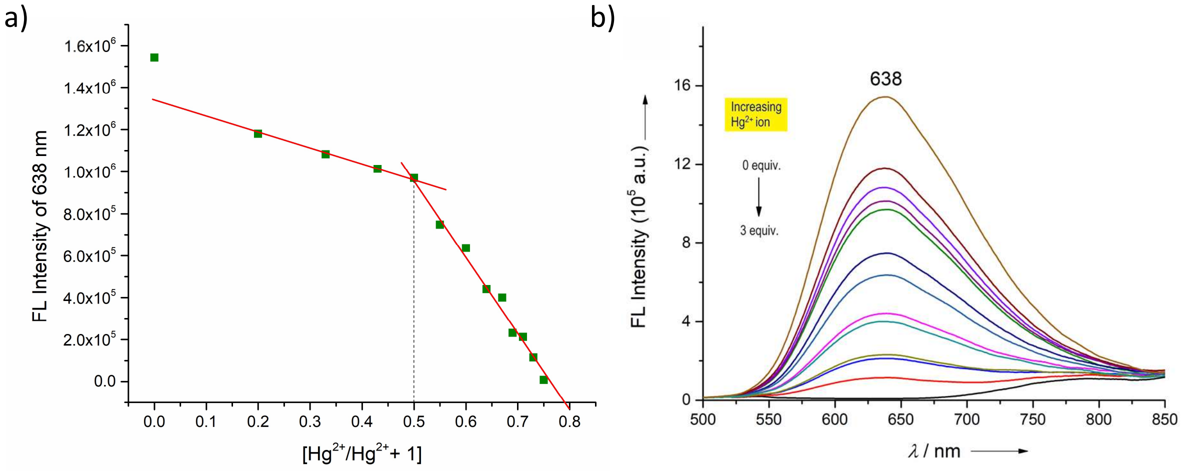

Figure S5-7. (a) Job’s plot for **1** with Hg^{2+} ions and (b) Emission intensity changes on Hg^{2+} addition (in $CHCl_3$).

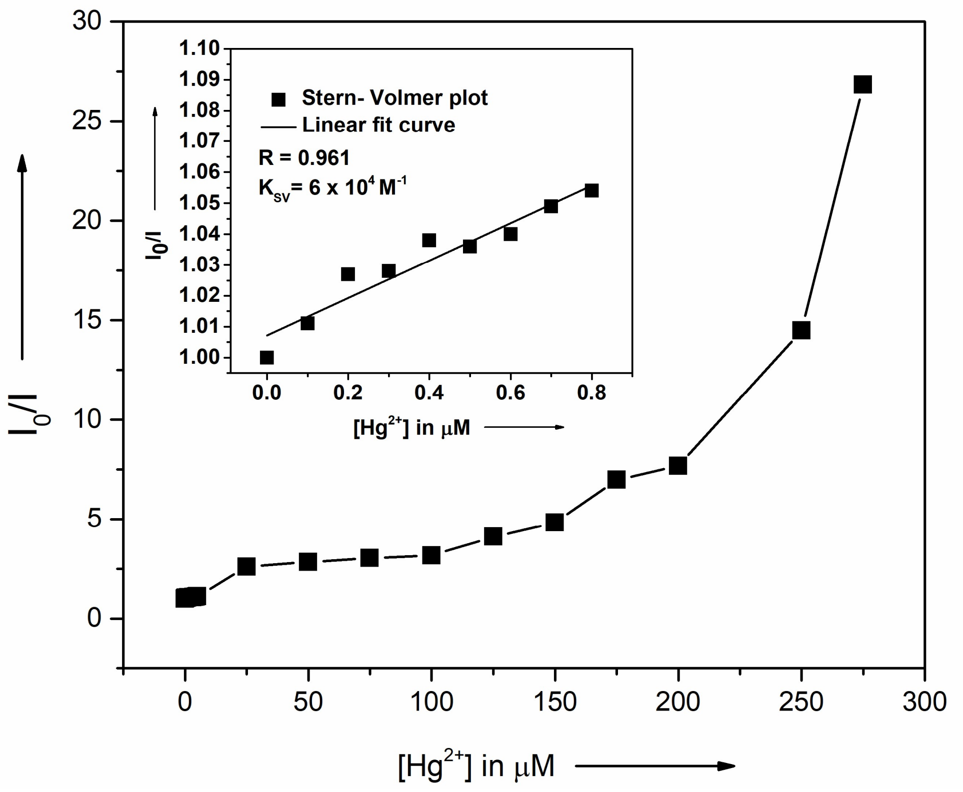

Figure S5-8. Stern-Volmer plot of **8** with different concentrations of Hg^{2+} (in $CHCl_3$).

4. Crystal Data: Bond parameters

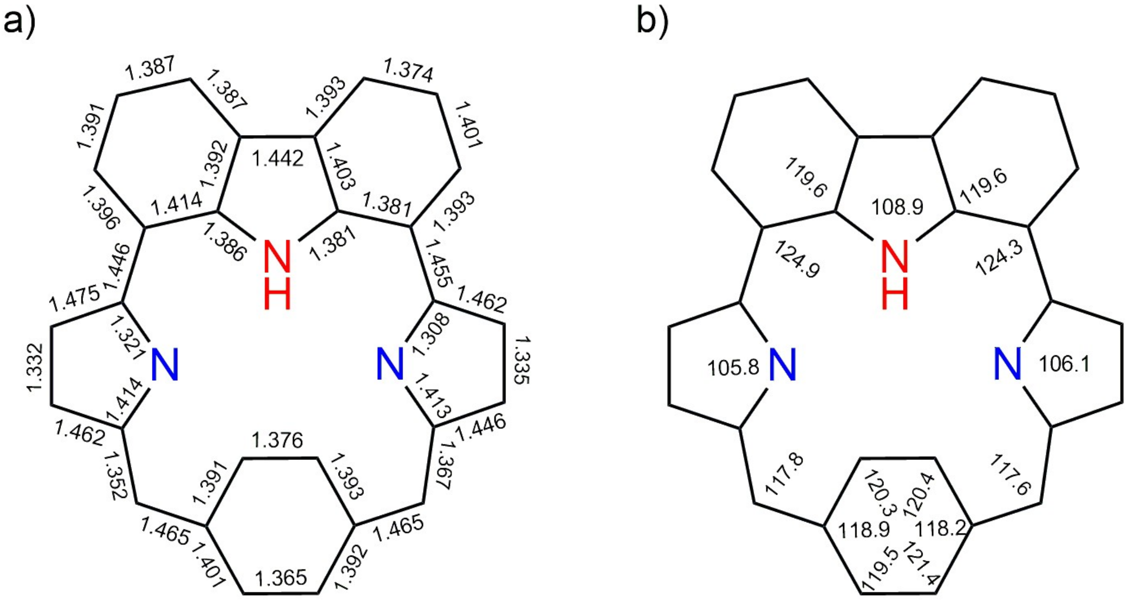

Figure S6-1. Detailed structural data for **1** (a) Selected bond lengths (Å) and (b) selected bond angles (°) are shown.

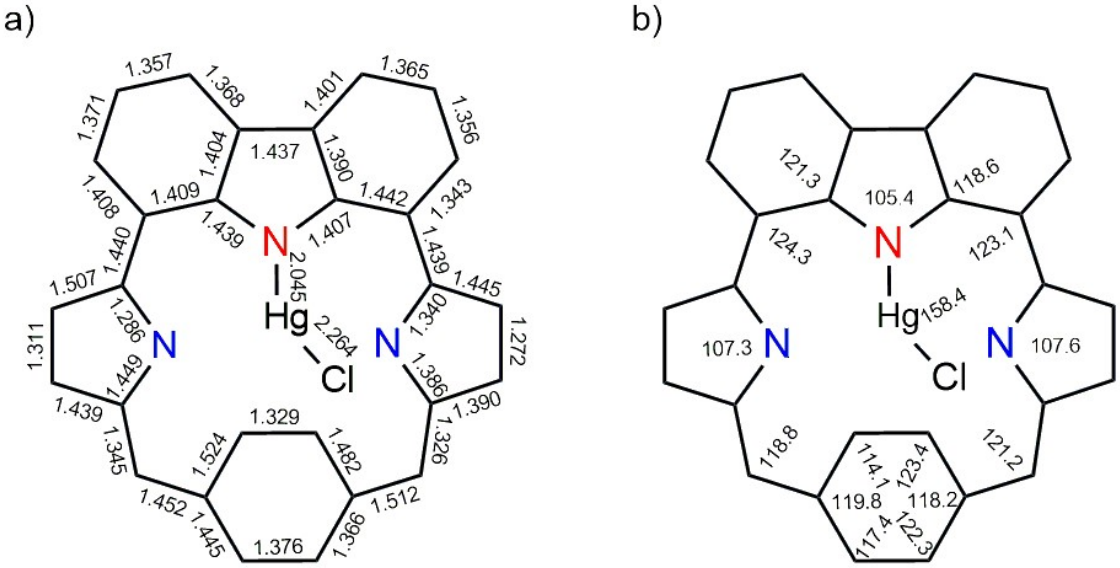

Figure S6-2. Detailed structural data for **1-Hg** (a) Selected bond lengths (Å) and (b) selected bond angles (°) are shown.

Method of Crystallization

Diffraction-grade crystals of **1** were grown by vapor diffusion of hexane into a $CHCl_3$ solution of **1** and **1-Hg** were grown by vapor diffusion of methanol into a $CHCl_3$ solution of **1-Hg** at room temperature

Table S6-1. Crystal data and structure refinements for **1** and **1-Hg**

Compound	**1**	**1-Hg**
Empirical formula	$C_{54} H_{53} N_3$	$C_{56} H_{54} Cl_7 Hg N_3$
Formula weight	743.99	1217.76
Temperature/*K*	140(2) *K*	140(2) K
Crystal system	Triclinic	Trigonal
Space group	*P -1*	R -3 :H
a/Å	10.502(3)	43.456(10)
b/Å	11.537(4)	43.456(10)
c/Å	19.141(6)	14.847(4)
α/°	96.877(12)	90
β/°	98.170(12)	90
γ/°	99.193(11)	120
Volume/Å^3	2242.0(12)	24281(13)
Z	2	18
ρ_{calc}g/cm^3	1.102	1.499
μ/mm^{-1}	0.064	3.238
F(000)	796	10980
Crystal size/mm^3	0.110 x 0.050 x 0.038	0.110 x 0.095 x 0.070
Radiation	Mo*Kα* (λ = 0.71073)	Mo*Kα* (λ = 0.71073)
2Θ range for data collection/°	1.991 to 25.000	0.937 to 24.998
Index ranges	-12≤ h≤ 12, -13≤ k≤ 13, -22≤ l≤ 22	-51<=h<=47, -48<=k<=51, -17<=l<=17
Reflections collected	49825	57481
Independent reflections	7880 [R(int) = 0.1946]	6494 [R(int) = 0.2144]
Data/restraints/parameters	7880 / 0 / 526	9494 / 44 / 614
Goodness-of-fit on F^2	1.014	1.009
Final *R* indexes [*I*>=2σ (*I*)]	R1 = 0.0753, wR2 = 0.1764	R1 = 0.0926, wR2 = 0.2415
Final *R* indexes [all data]	R1 = 0.1869, wR2 = 0.2343	R1 = 0.2334, wR2 = 0.3426
Largest diff. peak/hole / e Å^{-3}	0.390 / -0.309	0.926 and -0.706
CCDC Number	2350793	2350794

4.1 Secondary Interactions

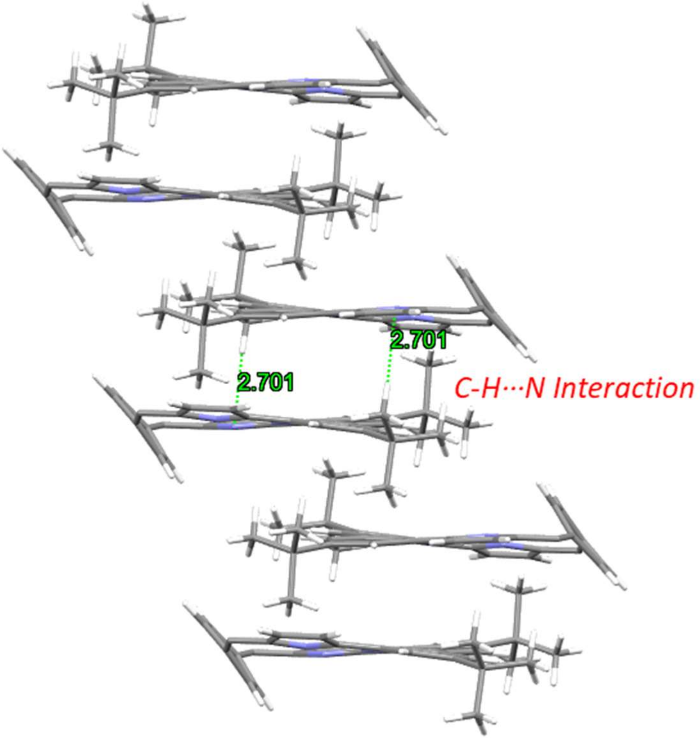

Figure S6-3. Crystal packing of **1** showing intermolecular C-H···N interactions.

5. DFT Calculations

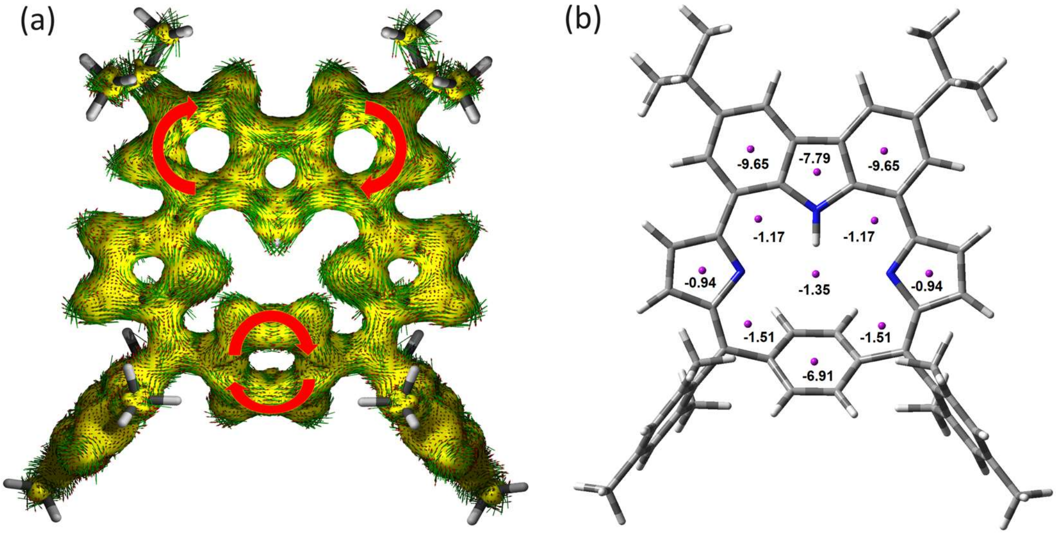

Figure S7-1. AICD plot and NICS(0) values of **1**.

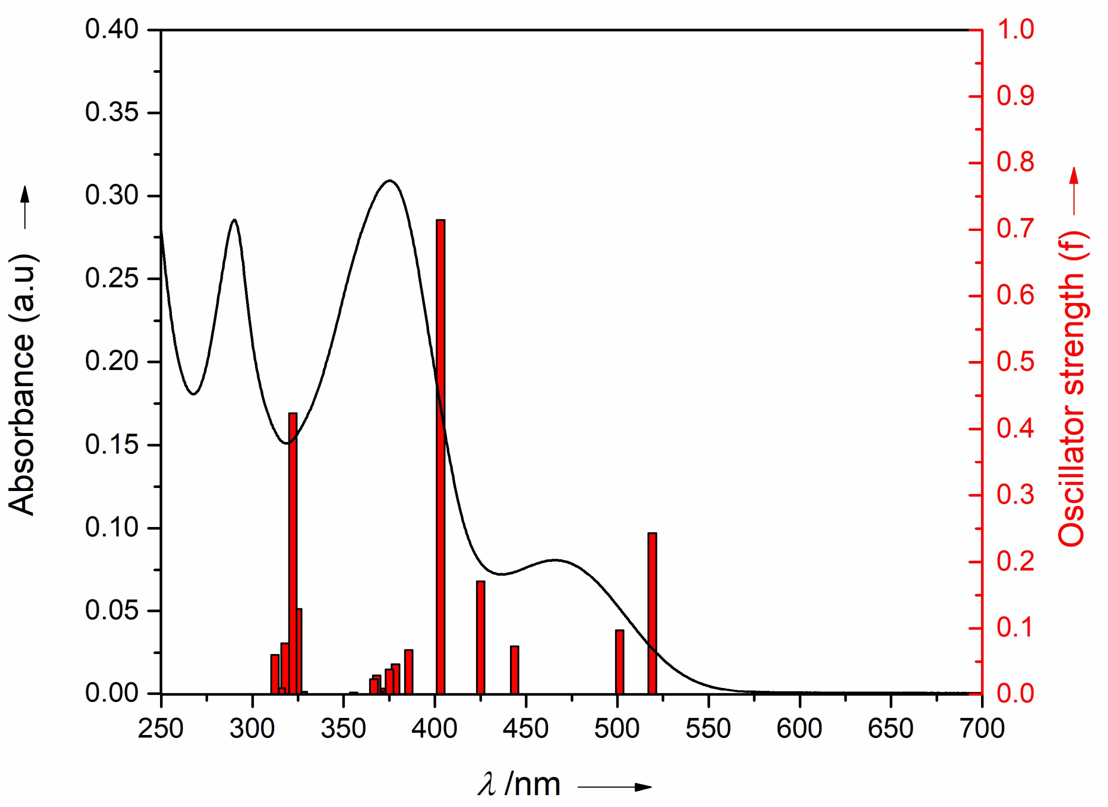

Figure S7-2. Calculated oscillator strength based on optimized structure (bar) and observed absorption spectra (line) of **1.**

Table S7-1: Selected transitions, oscillator strength, symmetry calculated for **1** from DFT analysis at B3LYP/6-311G(d) level of theory (H = HOMO, L= LUMO)

No.	Energy (cm^{-1})	Wavelength (nm)	Osc. Strength	Symmetry	Major contributions
1	19263.37	519.12	0.2432	Singlet-A	H→L (69.2%)
2	19948.93	501.28	0.0969	Singlet-A	H-1→L (67.4%), H→L+1 (18.5%)
3	22540.80	443.64	0.0727	Singlet-A	H-2→L (51.2%), H-1→L (17.3%)
4	23521.66	425.14	0.1703	Singlet-A	H-2→L (47.7%), H→L+1 (50.5%)
5	24807.12	403.11	0.7142	Singlet-A	H-1→L+1 (66.4%), H→L (11.7%)
6	25927.56	385.69	0.0671	Singlet-A	H-4→L+1 (12.4%), H-3→L (67.7%)
7	26426.36	378.41	0.0457	Singlet-A	H-6→L (22.1%),

					H-5→L (21.4%), H-4→L (58.9%), H-3→L+1 (19.9%)
8	26656.00	375.15	0.0383	Singlet-A	H-9→L (17.5%), H-8→L (53.9%), H-4→L (12.2%), H-2→L+1 (20.7%), H-1→L+1 (13.5%)
9	26981.81	370.62	0.0094	Singlet-A	H-5→L (43.7%)
10	27070.19	369.41	0.0048	Singlet-A	H-9→L (11.0%), H-8→L (24.7%), H-6→L (38.1%), H-5→L (39.2%), H-5→L+1 (11.2%)
11	27172.43	368.02	0.0292	Singlet-A	H-7→L (60.1%), H-5→L+1 (18.6%)
12	27279.92	366.57	0.0234	Singlet-A	H-10→L (10.3%), H-2→L+1 (64.1%), H→L+2 (13.1%)
13	28133.35	355.45	0.0024	Singlet-A	H-9→L (55.7%)
14	29494.17	339.05	0.0001	Singlet-A	H-13→L+1 (13.1%), H-12→L (31.2%), H-9→L+1 (16.0%), H-8→L+1 (44.8%)
15	30508.27	327.78	0.0038	Singlet-A	H-3→L+1 (65.7%)
16	30789.12	324.79	0.1289	Singlet-A	H→L+2 (63.2%)
17	31040.48	322.16	0.4239	Singlet-A	H-10→L (51.1%), H-9→L (25.7%), H-5→L+1 (11.9%), H-4→L+1 (20.8%)
18	31453.46	317.93	0.0772	Singlet-A	H-7→L+1 (15.8%), H-6→L+1 (19.2%), H-5→L+1 (11.8%),

					H-4→L+1 (55.2%)
19	31636.56	316.09	0.0026	Singlet-A	H-6→L (11.7%), H-6→L+1 (33.5%), H-5→L+1 (51.7%)
20	31664.61	315.81	0.0101	Singlet-A	H-6→L (12.2%), H-6→L+1 (54.5%)
21	32015.37	312.35	0.0599	Singlet-A	H-11→L (50.3%), H-9→L+1 (32.2%), H-8→L+1 (28.2%), H-3→L+1 (10.4%)

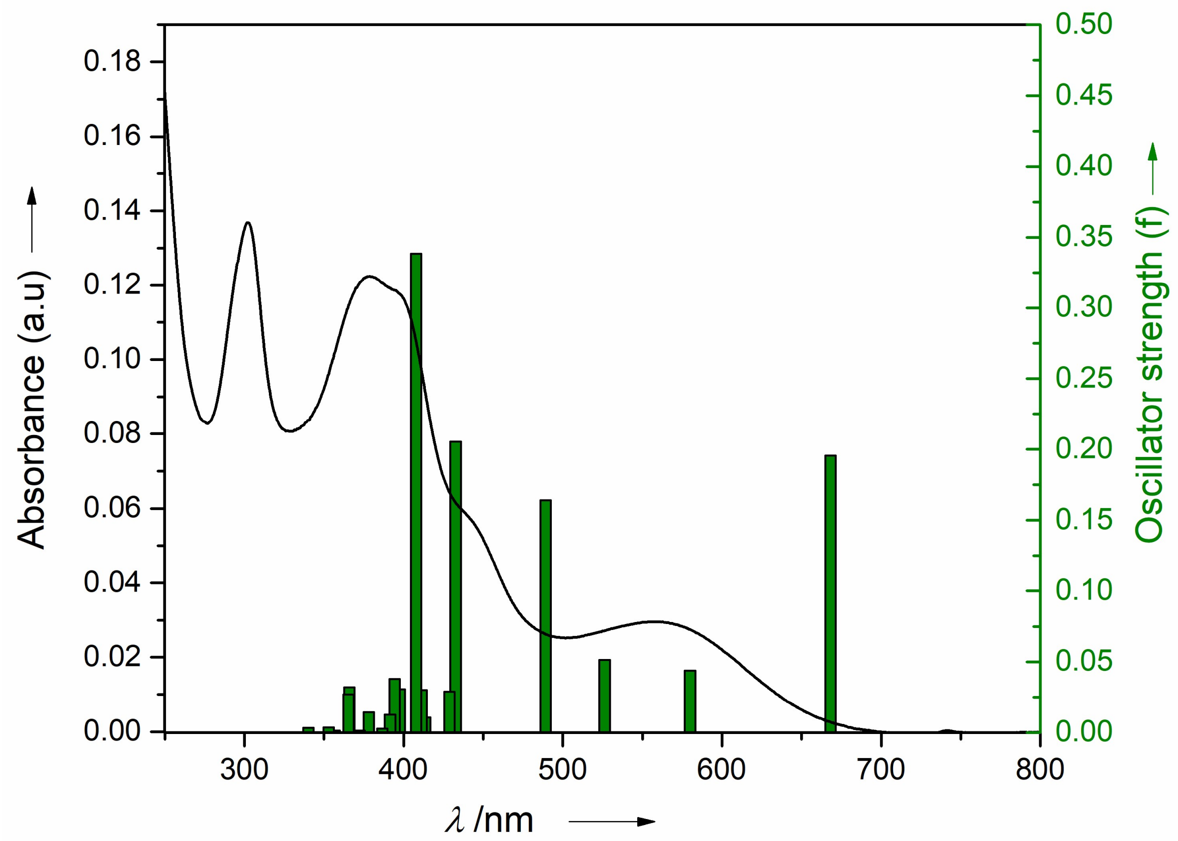

Figure S7-3. Calculated oscillator strength on the basis of optimized structure (bar) and observed absorption spectra (line) of **1- Hg**.

Table S7-2: Selected transitions, oscillator strength, symmetry calculated for **1-Hg** from DFT analysis atB3LYP/6-31G(d) level of theory (H = HOMO, L= LUMO)

No.	**Energy (cm^{-1})**	**Wavelength (nm)**	**Osc. Strength**	**Symmetry**	**Major contributions**
1	14968.49	668.07	0.1956	Singlet-A	H→L (69.2%)
2	17244.65	579.89	0.0436	Singlet-A	H-1→L (26.0%), H→L+1 (63.2%)
3	19001.65	526.27	0.0514	Singlet-A	H-2→L (37.2%), H-1→L (58.1%)
4	20445.72	489.10	0.1641	Singlet-A	H-2→L (57.2%), H→L+1 (27.1%)
5	23113.91	432.64	0.2054	Singlet-A	H-2→L+1 (24.0%), H-1→L+1 (58.2%)
6	23318.72	428.84	0.0288	Singlet-A	H-4→L (45.0%), H-3→L (41.4%), H-2→L+1 (20.4%), H-1→L+1 (21.6%)
7	24182.63	413.52	0.0106	Singlet-A	H-8→L (10.2%), H-7 →L (10.6%), H-5→L (64.5%), H-4→L (16.5%)
8	24320.25	411.18	0.0301	Singlet-A	H-5→L (17.8%), H-3→L (30.6%), H-2→L+1 (43.8%)
9	24526.03	407.73	0.3383	Singlet-A	H-12→L (17.2%), H-4→L (26.7%), H-2→L+1 (42.0%),
10	25154.70	397.54	0.0305	Singlet-A	H-7→L (12.2%), H-6→L (62.3%), H-3→L+1 (11.3%)
11	25359.47	394.33	0.0379	Singlet-A	H-7→L (60.8%)
12	25547.35	391.43	0.0125	Singlet-A	H-8→L (61.4%),

					H-7→L (22.2%), H-6→L (11.8%), H-6→L+1 (13.5%)
13	25869.87	386.55	0.0028	Singlet-A	H-10→L (28.7%), H-9→L (58.4%), H-7→L (10.2%), H-4→L (10.4%)
14	26451.53	378.05	0.0143	Singlet-A	H-10→L (55.6%)
15	26865.11	372.23	0.0012	Singlet-A	H-4→L+1 (49.5%), H-3→L+1 (43.7%)
16	27325.39	365.96	0.0319	Singlet-A	H-11→L (26.5%), H-10→L (19.6%), H→L+2 (59.0%)
17	27366.52	365.41	0.0270	Singlet-A	H-11→L (56.9%), H-9→L+1 (11.5%), H-4→L+1 (14.5%)
18	28044.98	356.57	0.0013	Singlet-A	H-8→L+1 (22.2%), H-7→L+1 (11.3%), H-5→L+1 (63.7%)
19	28338.25	352.88	0.0036	Singlet-A	H-11→L (15.9%), H-9→L+1 (14.3%), H-8→L (12.1%), H-3→L+1 (50.9%)
20	29198.79	342.48	0.0001	Singlet-A	H-13→L (13.7%), H-10→L+1 (22.2%), H-9→L+1 (31.1%), H-6→L+1 (46.8%), H-4→L+1 (24.2%)
21	29398.79	340.15	0.0032	Singlet-A	H-7→L+1 (32.6%), H-6→L+1 (44.2%)

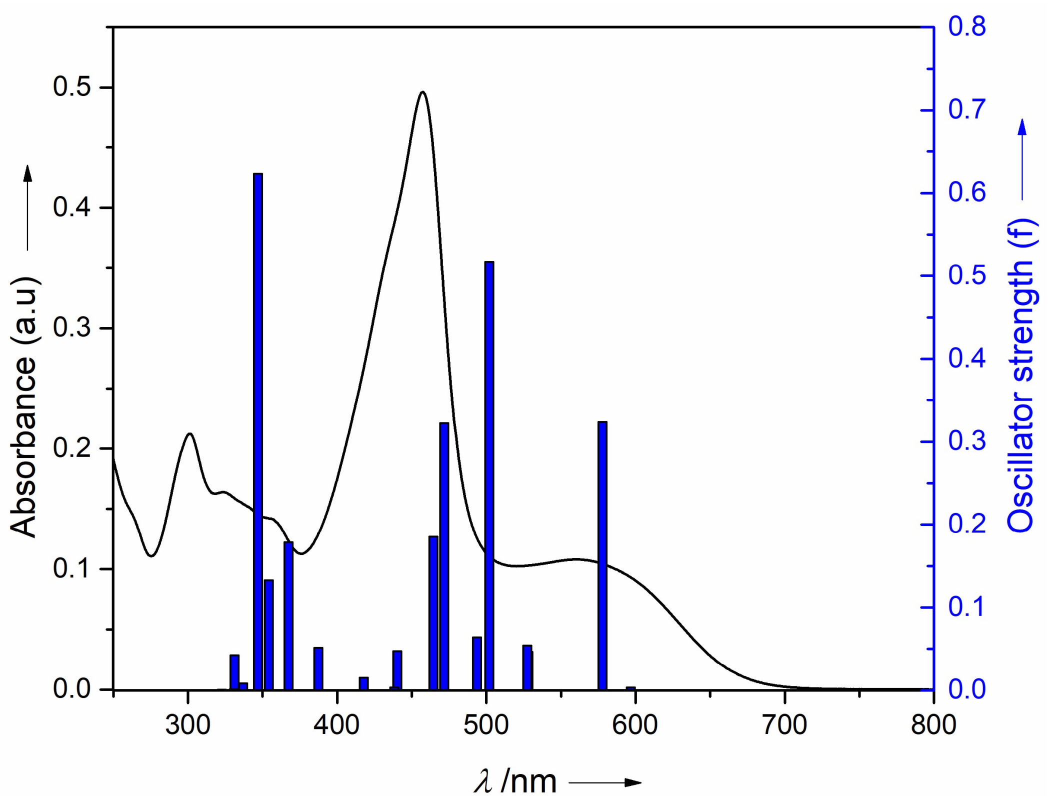

Figure S7-4. Calculated oscillator strength on the basis of optimized structure (bar) and observed absorption spectra (line) of **1·2H**$^+$.

Table S7-3: Selected transitions, oscillator strength, symmetry calculated for **1·2H**$^+$. from DFT analysis at B3LYP/6-31G(d) level of theory (H = HOMO, L= LUMO)

No.	**Energy (cm^{-1})**	**Wavelength (nm)**	**Osc. Strength**	**Symmetry**	**Major contributions**
1	16756.87	596.77	0.0034	Singlet-A	H→L (69.6%)
2	17310.32	577.69	0.3235	Singlet-A	H-1→L (68.9%), H→L+1 (13.0%)
3	18937.24	528.06	0.0466	Singlet-A	H-4→L (28.4%), H-2→L (54.2%)
4	18953.75	527.60	0.0039	Singlet-A	H-3→L (66.9%)
5	18962.38	527.36	0.0541	Singlet-A	H-4→L (47.4%), H-3→L+1 (16.3%)
6	19924.29	501.90	0.5173	Singlet-A	H-5→L (50.3%), H-1→L+1 (47.8%)
7	20255.22	493.70	0.0639	Singlet-A	H-4→L (43.1%),

					H-1→L+1 (53.6%)
8	21204.41	471.60	0.3224	Singlet-A	H→L+1 (49.1%)
9	21533.62	464.39	0.1855	Singlet-A	H-6→L (64.8%), H-5→L+1 (26.0%)
10	22710.75	440.32	0.0475	Singlet-A	H-4→L+1 (64.0%), H-2→L+1 (27.1%)
11	22818.55	438.24	0.0005	Singlet-A	H-3→L+1 (66.8%), H-2→L (21.8%)
12	22822.71	438.16	0.0035	Singlet-A	H-3→L (22.0%), H-2→L+1 (61.3%)
13	23934.32	417.81	0.0150	Singlet-A	H-5→L+1 (65.2%)
14	25822.44	387.26	0.0515	Singlet-A	H-7→L (19.8%), H-6→L+1 (66.5%)
15	27219.77	367.38	0.1784	Singlet-A	H-9→L (49.1%), H-7→L (48.1%)
16	28229.45	354.24	0.1327	Singlet-A	H-8→L (67.1%), H-7→L+1 (15.6%)
17	28821.77	346.96	0.6234	Singlet-A	H-9→L (66.1%), H-6→L+1 (66.1%)
18	29670.95	337.03	0.0083	Singlet-A	H-10→L (16.2%), H-9→L+1 (41.2%), H-7→L+1 (53.2%)
19	30185.03	331.29	0.0427	Singlet-A	H-11→L+1 (19.4%), H-10→L (65.3%)
20	30234.32	330.75	0.0014	Singlet-A	H-11→L (64.8%), H-10→L+1 (19.2%), H-8→L+1 (15.5%), H-1→L+2 (10.2%),
21	30993.34	322.65	0.0009	Singlet-A	H-8→L+1 (60.0%), H-1→L+2 (30.1%)

8. Cartesian coordinates of optimized geometries and minimized energies

Table S8-1: Cartesian coordinates of the S0 optimized geometry of the macrocycle **1** optimized at B3LYP/6-311G(d) level of theory

Sum of imaginary frequencies = 0

Total Energy (hartree) = -2254.418475 Hartrees

Optimized structure Coordinates:

Chemical Symbol	Coordinates (Angstroms)		
	X	Y	Z
C	-2.78018	-1.133952	-0.040877
C	-4.134261	-0.720592	0.008465
C	-5.180566	-1.641773	0.050315
H	-6.199384	-1.275458	0.084855
C	-4.911493	-3.00862	0.047741
C	-3.564652	-3.39954	0.005941
H	-3.346044	-4.458978	-0.002853
C	-2.471063	-2.518854	-0.038712
C	-1.121383	-3.071803	-0.083299
C	-0.778565	-4.500065	0.05154
H	-1.461346	-5.325815	0.189372
C	0.569251	-4.574919	-0.006482
H	1.187516	-5.459645	0.047012
C	1.052081	-3.212615	-0.200882
C	2.359148	-2.811304	-0.31261
C	2.645814	-1.402836	-0.60225
C	1.841796	-0.688638	-1.508162
H	1.168933	-1.227549	-2.16049
C	1.841748	0.688046	-1.508375
H	1.168858	1.226699	-2.160887
C	2.64573	1.402588	-0.602708
C	3.614526	0.694511	0.128969
H	4.299653	1.233604	0.774336
C	3.614552	-0.694466	0.129213
H	4.299596	-1.233333	0.774854
C	2.359107	2.811185	-0.31365
C	1.052012	3.212545	-0.202164
C	0.569137	4.574897	-0.008271
H	1.187365	5.459667	0.044871
C	-0.778682	4.500033	0.049798
H	-1.461484	5.325819	0.187322
C	-1.121459	3.071716	-0.084505
C	-2.47112	2.518739	-0.039636
C	-3.564735	3.399412	0.004778
H	-3.346159	4.458854	-0.004385
C	-4.911562	3.008471	0.046786

C	-5.1806	1.641618	0.049806
H	-6.199407	1.275287	0.084508
C	-4.134275	0.72045	0.008221
C	-2.780202	1.133827	-0.041286
C	-6.01575	-4.081137	0.087568
C	-5.926048	-4.968502	-1.174589
H	-4.963874	-5.480889	-1.248048
H	-6.052143	-4.372506	-2.082533
H	-6.70726	-5.735238	-1.162334
C	-7.424133	-3.462544	0.133381
H	-8.176405	-4.255468	0.161153
H	-7.630947	-2.848634	-0.74759
H	-7.571112	-2.843299	1.022612
C	-6.015849	4.080967	0.086374
C	-5.841653	4.962513	1.343767
H	-5.906146	4.362344	2.25542
H	-6.621932	5.729025	1.387709
H	-4.876826	5.475099	1.35454
C	-5.926237	4.968006	-1.176018
H	-4.964084	5.480405	-1.249658
H	-6.707475	5.734718	-1.163924
H	-6.052358	4.371768	-2.083799
C	-7.424212	3.462345	0.132418
H	-7.631044	2.848184	-0.748374
H	-8.176506	4.255254	0.160003
H	-7.571137	2.843342	1.021826
C	3.483924	-3.753078	-0.033518
C	4.32159	-4.170774	-1.09244
C	5.372088	-5.044252	-0.822337
H	6.003079	-5.374861	-1.643838
C	5.637616	-5.505751	0.469676
C	4.810123	-5.070311	1.500696
H	5.004684	-5.408637	2.51524
C	3.732828	-4.205401	1.27748
C	4.07681	-3.710924	-2.510354
H	4.752401	-4.2129	-3.205497
H	4.228436	-2.63323	-2.617649
H	3.051672	-3.91821	-2.83029
C	6.796718	-6.436399	0.730748
H	6.752954	-7.319993	0.086844
H	6.810536	-6.780737	1.766862
H	7.754725	-5.944249	0.533416
C	2.884522	-3.777394	2.455067
H	3.434122	-3.904683	3.390263
H	1.968596	-4.371146	2.530251
H	2.573977	-2.73334	2.385049
C	3.483737	3.75314	-0.034552
C	4.324052	4.167399	-1.091839

C	5.377211	5.038294	-0.820434
H	6.012595	5.363485	-1.640581
C	5.640454	5.501541	0.470702
C	4.811615	5.066434	1.501687
H	5.00821	5.401632	2.516947
C	4.08358	3.704067	-2.509361
H	4.759538	4.206245	-3.204003
H	3.058726	3.908514	-2.831947
H	4.237828	2.626502	-2.614285
C	6.778667	6.45778	0.730962
H	6.511035	7.479684	0.440567
H	7.670923	6.185744	0.16065
H	7.051255	6.480679	1.78834
N	-1.983478	-0.000059	-0.074552
H	-0.972262	-0.000062	-0.110777
N	-0.044953	-2.333186	-0.231719
N	-0.045	2.333087	-0.232676
C	3.732678	4.204908	1.277359
C	2.884117	3.775295	2.45419
H	1.965134	4.364643	2.526134
H	3.431203	3.907351	3.390177
H	2.578757	2.729551	2.385879
C	-5.841589	-4.962351	1.345197
H	-4.876752	-5.474913	1.35615
H	-6.621849	-5.728872	1.3893
H	-5.906141	-4.361949	2.256693

Table S8-2: Cartesian coordinates of the S0 optimized geometry of the macrocycle **1** optimized at B3LYP/6-311G(d) level of theory

Sum of imaginary frequencies = 0

Total Energy (hartree) = -2255.145225 Hartrees

Optimized structure Coordinates:

Chemical Symbol	Coordinates (Angstroms)		
	X	Y	Z
C	-2.813337	-1.143944	0.183031
C	-4.143546	-0.72497	0.042734
C	-5.192193	-1.642235	-0.05149
H	-6.205112	-1.275818	-0.156843
C	-4.94095	-3.014978	0.001551
C	-3.605032	-3.414568	0.116672
H	-3.39293	-4.474653	0.116628

C	-2.508132	-2.52784	0.18623
C	-1.182107	-3.101977	0.162457
C	-0.798418	-4.479036	0.292685
H	-1.467702	-5.300322	0.491604
C	0.556035	-4.564022	0.12992
H	1.158664	-5.458992	0.149801
C	1.075179	-3.24878	-0.098655
C	2.380185	-2.83242	-0.274938
C	2.621862	-1.406574	-0.569979
C	1.857523	-0.692295	-1.514421
H	1.27028	-1.230056	-2.251479
C	1.857508	0.692368	-1.514412
H	1.270252	1.230126	-2.251462
C	2.621828	1.406652	-0.569958
C	3.532957	0.69494	0.226185
H	4.182809	1.233937	0.905753
C	3.532972	-0.694852	0.226176
H	4.182835	-1.233844	0.905738
C	2.380118	2.832489	-0.274902
C	1.075104	3.248828	-0.098639
C	0.555935	4.564063	0.129916
H	1.15855	5.459043	0.1498
C	-0.798527	4.479063	0.292604
H	-1.467834	5.300344	0.491468
C	-1.182184	3.101989	0.16243
C	-2.508196	2.527823	0.186197
C	-3.605116	3.414523	0.116608
H	-3.39304	4.474613	0.116546
C	-4.941024	3.014898	0.001485
C	-5.192233	1.642147	-0.051528
H	-6.205142	1.275704	-0.156878
C	-4.143563	0.724911	0.042719
C	-2.813366	1.143919	0.183017
C	-6.054419	-4.074512	-0.079386
C	-5.828073	-4.96133	-1.32538
H	-4.875713	-5.496789	-1.288609
H	-5.844745	-4.370067	-2.244599
H	-6.617317	-5.713051	-1.398758
C	-7.449724	-3.435137	-0.187446
H	-8.208074	-4.218781	-0.233296
H	-7.561059	-2.831715	-1.092758
H	-7.687932	-2.811147	0.678585
C	-6.054519	4.074403	-0.079477
C	-6.01862	4.949318	1.194534
H	-6.174661	4.350037	2.095223
H	-6.808947	5.702352	1.154503
H	-5.071078	5.482731	1.30714
C	-5.828213	4.961179	-1.325509

H	-4.875867	5.496666	-1.288771
H	-6.617478	5.712875	-1.398906
H	-5.844881	4.369879	-2.244704
C	-7.449811	3.434993	-0.187491
H	-7.561142	2.831522	-1.092772
H	-8.208178	4.218618	-0.233373
H	-7.687997	2.811041	0.678574
C	3.509441	-3.747072	-0.041753
C	4.44505	-3.964391	-1.094611
C	5.490515	-4.851457	-0.885279
H	6.181589	-5.046466	-1.699866
C	5.680854	-5.509647	0.337618
C	4.777309	-5.250572	1.366791
H	4.930958	-5.721266	2.333258
C	3.68712	-4.393546	1.209742
C	4.293354	-3.317386	-2.452344
H	4.978116	-3.768726	-3.170242
H	4.517125	-2.247165	-2.424745
H	3.282704	-3.430524	-2.854374
C	6.829195	-6.463203	0.520699
H	6.695612	-7.35381	-0.101549
H	6.925067	-6.792658	1.555707
H	7.775975	-6.006398	0.220263
C	2.820062	-4.140912	2.426684
H	3.442175	-4.090879	3.322207
H	2.102708	-4.95007	2.591738
H	2.25418	-3.210747	2.369249
C	3.509362	3.74716	-0.041717
C	4.444982	3.964457	-1.09456
C	5.490475	4.851491	-0.885213
H	6.181565	5.046479	-1.699792
C	5.680825	5.50966	0.337689
C	4.777257	5.250605	1.366853
H	4.930917	5.721286	2.333325
C	4.293296	3.31743	-2.452284
H	4.978016	3.768803	-3.170201
H	3.282631	3.4305	-2.854295
H	4.517134	2.247223	-2.424675
C	6.829197	6.463171	0.520808
H	6.695693	7.35377	-0.101468
H	7.775975	6.006314	0.220445
H	6.925022	6.792647	1.555814
N	-1.969187	-0.000001	0.25408
H	-1.264483	0.000013	0.984742
N	-0.050639	-2.399963	-0.05477
N	-0.050698	2.399992	-0.054753
C	3.68704	4.393624	1.209787
C	2.819942	4.141007	2.426703

H	2.102332	4.949983	2.591527
H	3.441983	4.091335	3.322294
H	2.254336	3.210662	2.369404
C	-6.018521	-4.949377	1.194659
H	-5.070972	-5.48277	1.307298
H	-6.808835	-5.702426	1.154647
H	-6.174583	-4.350064	2.095324
H	-0.030871	-1.423611	-0.304506
H	-0.030906	1.423631	-0.304456

Table S8-3: Cartesian coordinates of the S0 optimized geometry of the macrocycle **1-Hg** optimized at B3LYP/ LANL2DZ level of theory

Sum of imaginary frequencies = 0

Total Energy (hartree) = -2310.754325 Hartrees

Optimized structure Coordinates:

Chemical Symbol	Coordinates (Angstroms)		
	X	Y	Z
C	2.931212	1.123433	-0.152968
C	4.314571	0.727365	-0.16744
C	5.343264	1.675987	-0.168693
H	6.376626	1.344361	-0.177379
C	5.034122	3.055773	-0.155538
C	3.673304	3.429951	-0.155585
H	3.44123	4.489088	-0.158902
C	2.584136	2.512821	-0.163898
C	1.223512	3.042271	-0.22542
C	0.872137	4.477892	-0.247354
H	1.566753	5.30451	-0.217218
C	-0.49431	4.567837	-0.312172
H	-1.099474	5.462555	-0.363219
C	-1.01496	3.201911	-0.384438
C	-2.341792	2.820563	-0.547693
C	-2.648091	1.41701	-0.875236
C	-1.801492	0.696267	-1.762939
H	-1.100394	1.237007	-2.388507
C	-1.801299	-0.696573	-1.762905
H	-1.099993	-1.237126	-2.388395
C	-2.647734	-1.417489	-0.87518
C	-3.67407	-0.701921	-0.205844
H	-4.380101	-1.238589	0.42066
C	-3.674248	0.701212	-0.205867
H	-4.380404	1.23773	0.420625
C	-2.341197	-2.821015	-0.547681

C	-1.014305	-3.20223	-0.38461
C	-0.493414	-4.568067	-0.312489
H	-1.098454	-5.462869	-0.363561
C	0.873026	-4.477886	-0.247767
H	1.567803	-5.304375	-0.217773
C	1.224151	-3.042196	-0.225746
C	2.584673	-2.512505	-0.164213
C	3.67403	-3.429407	-0.15603
H	3.442188	-4.488595	-0.15947
C	5.034767	-3.054933	-0.15596
C	5.343621	-1.675079	-0.168936
H	6.376915	-1.343242	-0.177587
C	4.314732	-0.726668	-0.167558
C	2.931463	-1.12304	-0.153135
C	6.124607	4.154446	-0.147652
C	5.978534	5.049505	-1.414012
H	4.99646	5.53613	-1.457824
H	6.097806	4.453805	-2.328247
H	6.743585	5.838089	-1.414199
C	7.556503	3.561944	-0.144833
H	8.29124	4.377255	-0.13555
H	7.747771	2.953461	-1.038505
H	7.738574	2.941176	0.742214
C	6.125489	-4.153376	-0.148236
C	5.969868	-5.036852	1.125042
H	6.083059	-4.433096	2.034649
H	6.734182	-5.826049	1.137733
H	4.987007	-5.521963	1.166714
C	5.979572	-5.048305	-1.414707
H	4.997603	-5.535137	-1.458551
H	6.744795	-5.836721	-1.415018
H	6.098686	-4.452461	-2.32887
C	7.55726	-3.560571	-0.145379
H	7.748384	-2.951951	-1.038988
H	8.292168	-4.37573	-0.1362
H	7.739215	-2.939863	0.741734
C	-3.453737	3.792352	-0.31112
C	-4.299599	4.178334	-1.392201
C	-5.348603	5.083855	-1.154794
H	-5.981244	5.387642	-1.987488
C	-5.601695	5.607502	0.131223
C	-4.767423	5.200111	1.188229
H	-4.956416	5.579954	2.190456
C	-3.691527	4.305887	0.995559
C	-4.071792	3.654569	-2.800822
H	-4.712542	4.17845	-3.518506
H	-4.295265	2.582151	-2.873027
H	-3.029221	3.786009	-3.118369

C	-6.745498	6.578541	0.360764
H	-6.609853	7.497891	-0.225522
H	-6.823884	6.863103	1.415846
H	-7.706458	6.140778	0.058038
C	-2.854754	3.895493	2.198649
H	-3.364506	4.169934	3.128842
H	-1.876067	4.392691	2.199488
H	-2.658284	2.817305	2.228606
C	-3.453001	-3.7929	-0.310856
C	-4.298956	-4.179192	-1.391752
C	-5.347807	-5.084799	-1.154027
H	-5.980511	-5.388853	-1.986576
C	-5.600684	-5.608201	0.132135
C	-4.766328	-5.200505	1.188956
H	-4.955142	-5.580175	2.19128
C	-4.071383	-3.655638	-2.800485
H	-4.712107	-4.179752	-3.518022
H	-3.028819	-3.786935	-3.118111
H	-4.295057	-2.58327	-2.872848
C	-6.744473	-6.579174	0.362035
H	-6.6101	-7.497707	-0.225804
H	-7.705742	-6.140594	0.061449
H	-6.821355	-6.865216	1.416827
N	2.110182	0.000104	-0.140532
N	0.089919	2.299848	-0.29362
N	0.09042	-2.299991	-0.293845
C	-3.690575	-4.306174	0.99596
C	-2.853696	-3.895403	2.198853
H	-1.875004	-4.392583	2.199725
H	-3.363352	-4.169591	3.12918
H	-2.65731	-2.817193	2.228493
C	5.968762	5.037727	1.125736
H	4.985796	5.522622	1.167437
H	6.732909	5.827084	1.138553
H	6.082051	4.433877	2.035268
Hg	-0.012679	-0.000192	0.635346
Cl	-1.476958	0.00046	2.724053

9. Supporting References

[S1] Gaussian 16, Revision C.01, Frisch MJ, Trucks GW, Schlegel HB, Scuseria GE, Robb MA, Cheeseman JR, Scalmani G, Barone V, Petersson GA, NakatsujiH, Li X, Caricato M, Marenich AV, Bloino J, Janesko BG, Gomperts R, Mennucci B, Hratchian HP, Ortiz JV, Izmaylov AF, Sonnenberg JL, Williams-Young D, Ding F, Lipparini F, Egidi F, Goings J, Peng B, Petrone A, Henderson T, Ranasinghe D, Zakrzewski VG, Gao J, Rega N, Zheng G, Liang W, Hada M, Ehara M, Toyota K, Fukuda R, Hasegawa J, Ishida M, Nakajima T, Honda Y, Kitao O, Nakai H, Vreven T, Throssell K, Montgomery JA Jr, Peralta JE, Ogliaro F, Bearpark

M, Heyd JJ, Brothers EN, Kudin KN, Staroverov VN, Keith T, Kobayashi R, Normand J, Raghavachari K, Rendell A, Burant JC, Iyengar SS, Tomasi J, Cossi M, Millam J M, Klene M, Adamo C, Cammi R, Ochterski JW, Martin RL, Morokuma K, Farkas O, Foresman JB, Fox DJ. Gaussian, Inc., Wallingford CT, 2016.

[S2] (a) A. D. Becke, *J. Chem. Phys.,* 1993, **98**, 1372; (b) C. Lee, W. Yang and R. G. Parr, *Phys. Rev. B*, 1988, **37**, 785.

[S3] (a) R. Bauernschmitt, R. Ahlrichs, *Chem. Phys. Lett.* 1996, **256**, 454-464; (b) R. E. Stratmann, G. E. Scuseria, M. J. Frisch, *J. Chem. Phys.* 1998, **109**, 8218-8224; (c) M. E. Casida, C. Jamorski, K. C. Casida, D. R. Salahub, *J. Chem. Phys.* 1998, **108**, 4439-4449.

[S4] SADABS, SMART, SAINT, and SHELXTL, Bruker AXS Inc., Madison, Wisconsin, USA, 2000.

[S5] Spek, A. L. *Acta Cryst*. 2015, **C71**, 9–18

[S6] M. S. Mudadu, A. N. Singh and R. P. Thummel*, J. Org. Chem.,* 2008, **73**, 6513-6520.